J. Fluid Mech. (1987), *vol.* 178, *pp.* 325–343
Printed in Great Britain

Three-dimensional steady streaming in a uniform tube with an oscillating elliptical cross-section

By N. PADMANABHAN† AND T. J. PEDLEY

Department of Applied Mathematics and Theoretical Physics, University of Cambridge, Silver Street, Cambridge CB3 9EW, UK

(Received 5 June 1986 and in revised form 9 December 1986)

We analyse the steady streaming generated in an infinite elliptical tube containing a viscous, incompressible fluid when the boundary oscillates in such a way that the area and ellipticity of the cross-section vary with time but remain independent of the longitudinal coordinate. The parameters $\alpha^{-1} = (\nu/\Omega a_0^2)^{\frac{1}{2}}$ and $\epsilon = U_0/a_0\Omega$, where ν is the kinematic viscosity, Ω is the oscillation frequency, a_0 is the undisturbed semi-major axis and U_0 is a typical wall velocity, are taken to be small, so that the Stokes layer is thin and the interaction which leads to the steady streaming can be analysed as a small perturbation. Coupled axial and transverse velocities, both oscillatory and steady, are generated. A complication is the need to specify the tangential as well as the normal velocity component on the tube wall, which requires an assumption concerning its elastic properties. We have considered two cases: (i) constant major axis, in which all boundary points move parallel to the minor axis, and (ii) an inextensible wall. The three-dimensional steady streaming in the core of the tube is computed only in the limit of small steady-streaming Reynolds number, $R_s = \epsilon^2\alpha^2$.

1. Introduction

The work described in this paper arose from the study of oscillations in collapsible tubes such as blood vessels (Pedley 1980, Chapter 6). In certain conditions, large-amplitude, high-frequency oscillations in cross-sectional area and cross-sectional shape arise spontaneously at a certain location in a fluid-filled flexible tube, and these are coupled to oscillations in the emerging flow rate (Conrad 1969). A complete analysis of such oscillations is as yet an intractable problem, because of the great complexity of analysing either large, unsteady, three-dimensional deformations of an elastic cylinder or unsteady, three-dimensional, viscous flow in a non-uniform tube, and the even greater complexity when the two problems are combined. This paper is a contribution solely to the fluid mechanics, although a little thought has to be given to the elasticity.

The fluid is taken to be viscous and incompressible with kinematic viscosity ν. To simplify the fluid mechanics we consider: (*a*) a tube with uniform cross-section (i.e. independent of the longitudinal coordinate z), with the consequence that flow separation is suppressed, although it is believed to be most important in real collapsible-tube oscillations (Cancelli & Pedley 1985); (*b*) a tube with elliptical cross-section, which is known to be a good approximation for a partially collapsed

† Permanent address: Centre for Atmospheric and Fluids Science, Indian Institute of Technology-Delhi, Hauz Khas, New Delhi 110016, India.

tube (Moreno *et al.* 1970); (*c*) small-amplitude oscillations. Because the cross-sectional area is not constant in time, an oscillatory axial flow is generated, with a velocity whose magnitude is proportional to z, measured from a cross-section across which there is zero flow rate. Moreover, because the cross-sectional shape is not constant, transverse oscillatory motions are also generated, and these are coupled to the axial flow through the continuity equation as well as the axial momentum equation, so the flow is three-dimensional. If the frequency Ω is sufficiently high (i.e. $\alpha^2 = \Omega a_0^2/\nu \gg 1$, where a_0 is a typical tube diameter), these primary oscillations can be analysed in two regions, an inviscid core and a viscous (Stokes) boundary layer. Because the boundary-layer problem is nonlinear, a non-zero mean flow, or steady streaming, is generated at second order in an expansion in powers of amplitude. As is well-known, the tangential components of the steady-streaming velocity do not tend to zero at the edge of the boundary layer, and they drive a non-zero mean flow in the core. This is a Stokes flow if the steady-streaming Reynolds number R_s is small, and may have a tractable asymptotic form if R_s is large.† Such steady streaming has been familiar for many years in both internal and external flow (Rayleigh 1883; Riley 1967; Lyne 1971), but as far as the authors are aware this is the first genuinely three-dimensional case to be analysed (even this problem is not fully general because the z-dependence of the variables is very simple).

The corresponding two-dimensional and axisymmetric problems were solved by Secomb (1978). He showed that the (axial) steady-streaming velocity at the edge of the Stokes layer was directed in the direction of decreasing $|z|$, inwards from the far ends of the channel. There has to be a corresponding outflow near the centreplane of the channel by conservation of mass. Thus mean vorticity, generated at the wall, tends to accumulate near $z = 0$ and to be swept away again in the centre. The consequence is that, even at large values of R_s, mean vorticity is distributed across the whole cross-section and the flow cannot be described by boundary-layer theory, unlike most external steady-streaming flows (Riley 1967). Interestingly, Secomb predicted (in the two-dimensional case) that the profile of mean axial velocity does not depend strongly on R_s, being proportional to $z\cos\pi y/a$ in the limit $R_s \to \infty$ and to $\frac{1}{2}z(1-3y^2/a^2)$ in the limit $R_s \to 0$ (here y is the cross-channel coordinate and the mean wall positions are at $y = \pm a$). One of the aims of the present paper is to predict the direction of the steady-streaming velocity at the edge of the Stokes layer: is the axial component always negative, i.e. directed towards $z = 0$ as in Secomb's analysis, or are there cases where it is positive? It turns out that, in general, this velocity component has a different sign at different positions round the tube wall. It also turns out that simple analytical formulae for the steady-streaming velocity profiles outside the Stokes layer are not in general available even for small R_s.

The primary inviscid core flow, and hence the oscillatory tangential components of the velocity at the outer edge of the Stokes layer, are determined entirely by the normal component of the wall velocity. However, the transverse velocity components in the Stokes layer also depend on the tangential component of the wall velocity. This proves to be a major difficulty, for in order to specify this component it is in general necessary to solve a problem in dynamic elasticity, and the fluid mechanics cannot

† α_0 is generally large both for self-excited oscillations in collapsible tubes (Conrad 1969; $\alpha^2 \approx 20$–40) and for the pulse wave in arteries (e.g. $\alpha^2 \approx 170$ for the fundamental frequency in the human aorta, $\alpha^2 \approx 5$ in coronary arteries, which suffer periodic compression during contraction of the cardiac muscle). Thus a sufficiently small but still measurable amplitude of oscillation may render R_s of order 1 or less: R_s is defined in (4.1) below as $\epsilon^2\alpha^2$, where ϵ is the ratio of the amplitude of wall displacement to a_0.

be uncoupled from the solid mechanics. To overcome this we here examine only two relatively simple cases. In one the major axis of the ellipse is held constant while the minor axis varies (not a bad approximation for veins according to Moreno *et al.* (1970, figure 8), but the problem is further simplified by requiring every element of the wall to move parallel to the minor axis. The other case is a rational approximation for a wall consisting of a thin membrane with large Young's modulus: the tube wall is taken to be inextensible, so that not only the perimeter but also every material element of the wall keeps the same length throughout the oscillation.

An outline of the paper is as follows. The problem is formulated in §2, and the dimensionless velocity components are specified both in Cartesian coordinates and in a curvilinear coordinate system suitable for boundary-layer analysis, in which the transverse coordinates reduce, near the wall, to distance along and normal to the wall. Solutions for the inviscid core and the Stokes layer are derived in §3, culminating in a prediction of the tangential steady-streaming velocity at the edge of that layer. The core steady-streaming problem is defined in §4, while the wall motions are specified, and the core boundary conditions computed, in §5. In §6 the core problem is solved numerically in the limit of small R_s, and the results are discussed. Finally in §7 the as yet unsolved large-R_s problem is formulated, and future extensions of the present work are discussed.

2. Formulation

The equation of the elliptical tube wall in Cartesian coordinates (figure 1) is taken to be

$$F(x,y,t) \equiv \frac{x^2}{a^2(t)} + \frac{y^2}{b^2(t)} - 1 = 0, \tag{2.1}$$

where $2a$ is the major axis and $2b$ the minor axis. Elements of the wall are taken to move only in the transverse direction, so that a typical element (X, Y, Z) satisfying $F(X, Y, t) = 0$ has velocity $(\dot{X}, \dot{Y}, 0)$. We shall also need to know the intrinsic coordinates (s, ψ) of the element in the (x, y)-plane, as well as the normal $(u_{n\mathrm{w}})$ and tangential $(u_{s\mathrm{w}})$ components of its velocity; the senses of n and s are shown on figure 1. It is convenient to specify the position of the element (X, Y) in terms of its eccentric angle θ, so that

$$X(t) = a(t)\cos\theta(t), \quad Y(t) = b(t)\sin\theta(t); \tag{2.2}$$

moreover the intrinsic coordinates are given by

$$\tan\psi = \frac{b}{a}\cot\theta, \tag{2.3}$$

$$s = \int_0^\theta (a^2\sin^2\theta' + b^2\cos^2\theta')^{\frac{1}{2}}\,\mathrm{d}\theta'. \tag{2.4}$$

In terms of a, b, θ and their time derivatives, the normal and tangential velocity components of the element are

$$u_{n\mathrm{w}} = -(\dot{X}\sin\psi + \dot{Y}\cos\psi) = -\frac{(\dot{a}b\cos^2\theta + \dot{b}a\sin^2\theta)}{c}, \tag{2.5}$$

$$u_{s\mathrm{w}} = -\dot{X}\cos\psi + \dot{Y}\sin\psi = c\dot{\theta} + \frac{(b\dot{b} - a\dot{a})\sin\theta\cos\theta}{c}, \tag{2.6}$$

where

$$c = (a^2\sin^2\theta + b^2\cos^2\theta)^{\frac{1}{2}}. \tag{2.7}$$

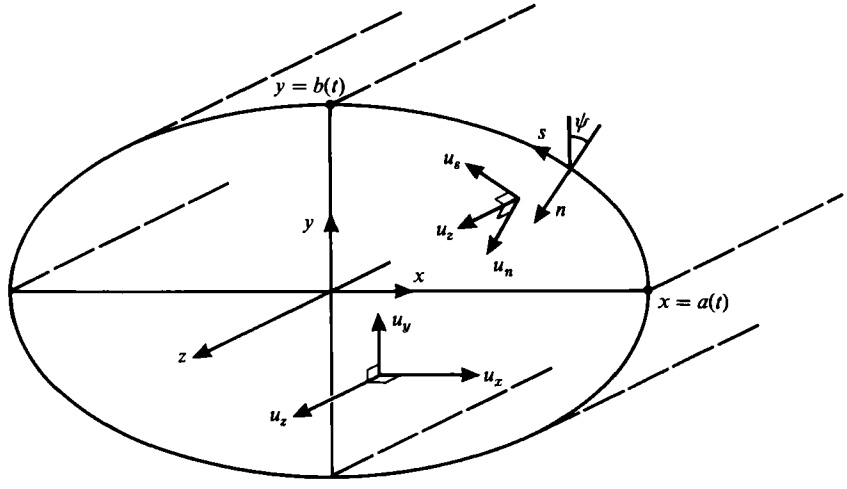

FIGURE 1. Definitions of coordinate systems and velocity components.

As shown by Secomb (1978) we can analyse the fluid motion driven by the wall motions independently of any net through flow driven by an applied pressure gradient, and we therefore seek a solution in which the axial velocity u_z is proportional to z while the transverse velocities are independent of z. Thus in Cartesian coordinates we take

$$\left.\begin{aligned} u_x = u_x(x,y,t), \quad u_y = u_y(x,y,t), \quad u_z = z w_1(x,y,t), \\ p = p_0(x,y,t) + \tfrac{1}{2} z^2 p_2(t), \end{aligned}\right\} \tag{2.8}$$

where p is the pressure, and the Navier–Stokes equations reduce to

$$\frac{\partial u_x}{\partial t} + u_x \frac{\partial u_x}{\partial x} + u_y \frac{\partial u_x}{\partial y} = -\frac{1}{\rho}\frac{\partial p_0}{\partial x} + \nu\left(\frac{\partial^2 u_x}{\partial x^2} + \frac{\partial^2 u_x}{\partial y^2}\right), \tag{2.9}$$

$$\frac{\partial u_y}{\partial t} + u_x \frac{\partial u_y}{\partial x} + u_y \frac{\partial u_y}{\partial y} = -\frac{1}{\rho}\frac{\partial p_0}{\partial y} + \nu\left(\frac{\partial^2 u_y}{\partial x^2} + \frac{\partial^2 u_y}{\partial y^2}\right), \tag{2.10}$$

$$\frac{\partial w_1}{\partial t} + u_x \frac{\partial w_1}{\partial x} + u_y \frac{\partial w_1}{\partial y} + w_1^2 = -\frac{1}{\rho} p_2 + \nu\left(\frac{\partial^2 w_1}{\partial x^2} + \frac{\partial^2 w_1}{\partial y^2}\right), \tag{2.11}$$

$$\frac{\partial u_x}{\partial x} + \frac{\partial u_y}{\partial y} + w_1 = 0, \tag{2.12}$$

where ρ is the fluid density. The boundary conditions are that $w_1 = 0$ and u_x and u_y are given on the wall. Although there are only two independent space variables and w_1 does not appear in (2.9) and (2.10), the problem for u_x and u_y is not one of two-dimensional flow because these components are coupled to w_1 through the continuity equation (2.12).

We are interested in solving the problem for high-frequency, small-amplitude oscillations of the wall, so to first order in the amplitude there will be an inviscid core with thin Stokes layers at the wall. The inviscid core flow is a solution of (2.9)–(2.12) with $\nu = 0$, and the only boundary condition to be satisfied is that the normal

component of the fluid's velocity at the wall is equal to that of the wall, $u_{n\mathrm{w}}$ (equation (2.5)). Solution of the inviscid problem will lead to predictions of tangential velocities

$$u_s = u_{s\mathrm{E}}, \quad w_1 = w_{1\mathrm{E}} \tag{2.13}$$

at the wall, where the suffix E represents the fact that these are the external values to which the velocities in the Stokes layer must tend. On the wall itself we have

$$u_s = u_{s\mathrm{w}}, \quad w_1 = 0. \tag{2.14}$$

In order to analyse the Stokes layer in a systematic way, it is advantageous to work in a moving orthogonal coordinate system, attached to the wall. In the boundary layer, the coordinates are s, the arclength measured along the wall, n, the distance normal to the wall, and z, with corresponding velocity components $u_s(s,n,t)$, $u_n(s,n,t)$ and $u_z = zw_1(s,n,t)$ (see figure 1). The full Navier–Stokes equations in this coordinate system are very complex but are a straightforward extension of the two-dimensional equations given by Longuet-Higgins (1953). Here we write the form they take under the boundary-layer approximation, with the following non-dimensionalization in which a transverse lengthscale is a_0, a wall velocity scale is U_0, and a frequency scale is Ω:

$$\left.\begin{gathered} s' = \frac{s}{a_0}, \quad n' = \frac{\alpha n}{a_0}, \quad t' = \Omega t, \\ u = \frac{u_s}{U_0}, \quad v = \frac{\alpha(u_n - u_{n\mathrm{w}})}{U_0}, \quad w = \frac{w_1 a_0}{U_0}, \\ u_{\mathrm{E}} = \frac{u_{s\mathrm{E}}}{U_0}, \quad u_{\mathrm{w}} = \frac{u_{s\mathrm{w}}}{U_0}, \quad w_{\mathrm{E}} = \frac{w_{1\mathrm{E}} a_0}{U_0}, \quad v_{\mathrm{w}} = \frac{u_{n\mathrm{w}}}{U_0}, \\ \kappa = \hat{\kappa} a_0, \end{gathered}\right\} \tag{2.15}$$

where $\hat{\kappa}$ is the wall curvature. We introduce two dimensionless parameters,

$$\alpha = a_0\left(\frac{\Omega}{\nu}\right)^{\frac{1}{2}}, \quad \epsilon = \frac{U_0}{a_0 \Omega}, \tag{2.16}$$

the former being the (Womersley) frequency parameter ($\alpha \gg 1$) and the latter the amplitude parameter ($\epsilon \ll 1$). The boundary-layer equations are (dropping the primes on s, n, t)

$$\frac{\partial u}{\partial t} + \epsilon\left[(u-u_{\mathrm{w}})\frac{\partial u}{\partial s} + v\frac{\partial u}{\partial n} + \kappa v_{\mathrm{w}} u\right] = \frac{\partial u_{\mathrm{E}}}{\partial t} + \epsilon\left[(u_{\mathrm{E}}-u_{\mathrm{w}})\frac{\partial u_{\mathrm{E}}}{\partial s} + \kappa v_{\mathrm{w}} u_{\mathrm{E}}\right] + \frac{\partial^2 u}{\partial n^2}, \tag{2.17}$$

$$\frac{\partial w}{\partial t} + \epsilon\left[(u-u_{\mathrm{w}})\frac{\partial w}{\partial s} + v\frac{\partial w}{\partial n} + w^2\right] = \frac{\partial w_{\mathrm{E}}}{\partial t} + \epsilon\left[(u_{\mathrm{E}}-u_{\mathrm{w}})\frac{\partial w_{\mathrm{E}}}{\partial s} + w_{\mathrm{E}}^2\right] + \frac{\partial^2 w}{\partial n^2}, \tag{2.18}$$

$$\frac{\partial u}{\partial s} + \frac{\partial v}{\partial n} + w = 0. \tag{2.19}$$

The boundary conditions are

$$\begin{gathered} u = u_{\mathrm{w}}(s,t), \quad v = w = 0 \quad \text{on } n = 0, \\ u \sim u_{\mathrm{E}}(s,t), \quad w \sim w_{\mathrm{E}}(s,t) \quad \text{as } n \to \infty, \end{gathered} \tag{2.20}$$

where $u_{\mathrm{w}}(s,t)$, for example, is evaluated at time t using (2.6) in which θ is determined by inverting (2.4) and $\dot{\theta}$ comes from differentiating (2.4) with $\dot{s}$ given by the nature of the wall elasticity.

3. Core and Stokes-layer solutions

3.1. *The inviscid core*

As stated earlier, the solution here depends only on the normal velocity of the wall, and must satisfy $\mathrm{D}F/\mathrm{D}t = 0$, where F is given by (2.1). It is readily verified that the (dimensional) solution of (2.12) that satisfies this condition is

$$u_x = \frac{x\dot{a}}{a}, \quad u_y = \frac{y\dot{b}}{b}, \quad w_1 = -\left(\frac{\dot{a}}{a}+\frac{\dot{b}}{b}\right); \tag{3.1}$$

the pressure terms p_0 and p_2 may be obtained by integrating (2.9)–(2.11). Transformation of (3.1) from the (x, y) coordinate system to the (s, n)-system gives the oscillatory, transverse, tangential velocity at the edge of the Stokes layer, $u_{s\mathrm{E}}$, as follows:

$$u_{s\mathrm{E}} = \frac{(b\dot{b}-a\dot{a})\sin\theta\cos\theta}{c}, \tag{3.2}$$

where c is given by (2.7), and θ is again obtained by inverting (2.4). The longitudinal velocity at the edge of the Stokes layer is, from (3.1), given by

$$w_{1\mathrm{E}} = -\left(\frac{\dot{a}}{a}+\frac{\dot{b}}{b}\right), \tag{3.3}$$

which we may note is independent of position on the boundary.

3.2. *Stokes layer*

Equation (3.1) is valid for all functions $a(t)$, $b(t)$. In analysing the boundary layer, however, we restrict attention to sinusoidal oscillations at large α and small ϵ. Large α means the Stokes layer has thickness small compared with a_0, and occupies a region in which $n = O(1)$; small ϵ means that we can expand the variables u, v, w (equation 2.15) in powers of ϵ. The leading-order terms will be linear solutions of the diffusion equation ((2.17) and (2.18) with $\epsilon = 0$), representing oscillations of dimensionless frequency 1, as in the classical Stokes layer. At the next order in ϵ there is, in addition to another forced term of frequency 1, a nonlinear interaction leading to oscillations of frequency 2 and to a non-zero mean term. We therefore write

$$u = \mathscr{R}\{u_0(s,n)\,\mathrm{e}^{\mathrm{i}t} + \epsilon[u_{10}(s,n) + u_{11}(s,n)\,\mathrm{e}^{\mathrm{i}t} + u_{12}(s,n)\,\mathrm{e}^{2\mathrm{i}t}] + O(\epsilon^2)\}, \tag{3.4}$$

with similar expressions for v and w; we also write

$$[u_{\mathrm{E}}, u_{\mathrm{w}}, w_{\mathrm{E}}, v_{\mathrm{w}}] = \mathscr{R}\{(u_{0\mathrm{E}}, u_{0\mathrm{w}}, w_{0\mathrm{E}}, \mathrm{v}_{0\mathrm{w}})\,\mathrm{e}^{\mathrm{i}t}\}, \tag{3.5}$$

where all the coefficients of $\mathrm{e}^{\mathrm{i}t}$ on the right of (3.5) are functions of s. The quantities of greatest interest are the (real) steady-streaming velocities u_{10} and w_{10}.

The solutions for the primary Stokes layer are

$$\left.\begin{aligned} u_0 &= u_{0\mathrm{E}}(s) + [u_{0\mathrm{w}}(s) - u_{0\mathrm{E}}(s)]\exp\left(-\frac{(1+\mathrm{i})}{\sqrt{2}}n\right), \\ w_0 &= w_{0\mathrm{E}}(s)\left[1-\exp\left(-\frac{(1+\mathrm{i})}{\sqrt{2}}n\right)\right], \\ v_0 &= -\int_0^n \left(\frac{\partial u_0}{\partial s}+w_0\right)\mathrm{d}n. \end{aligned}\right\} \tag{3.6}$$

Substitution of (3.5) and (3.6) into the $O(\epsilon)$-terms in (2.17) and (2.18) then yields the following problems for u_{10} and w_{10}:

$$\frac{\partial^2 u_{10}}{\partial n^2} = \frac{1}{4}\left\{(u_0-u_{0w})\frac{\partial u_0^*}{\partial s}-(u_{0E}-u_{0w})\frac{\partial u_{0E}^*}{\partial s}+v_0\frac{\partial u_0^*}{\partial n}+\kappa v_{0w}(u_0^*-u_{0E}^*)+\text{c.c.}\right\}, \quad (3.7)$$

$$\frac{\partial^2 w_{10}}{\partial n^2} = \frac{1}{4}\left\{(u_0-u_{0w})\frac{\partial w_0^*}{\partial s}-(u_{0E}-u_{0w})\frac{\partial w_{0E}^*}{\partial s}+v_0\frac{\partial w_0^*}{\partial n}+w_0 w_0^*-w_{0E}w_{0E}^*+\text{c.c.}\right\} \quad (3.8)$$

(where * and c.c. both mean complex conjugate), with boundary conditions $u_{10} = w_{10} = 0$ on $n = 0$, and u_{10}, w_{10} are bounded as $n\to\infty$ (as usual in steady-streaming problems it is not possible to impose the *a priori* reasonable conditions $u_{10}, w_{10}\to 0$ as $n\to\infty$).

Consider one term, with its complex conjugate, on the right-hand side of (3.7) or (3.8) and let its contribution to the solution be u_{10} (or w_{10}) $= q(s,n)$. Now any such term except one involving v_0 (e.g. $\frac{1}{4}u_0\,\partial u_0^*/\partial s$) can be written in the form

$$\left[A(s)+B(s)\exp\left(-\frac{(1+\mathrm{i})}{\sqrt{2}}n\right)\right]\left[C^*(s)+D^*(s)\exp\left(-\frac{(1-\mathrm{i})}{\sqrt{2}}n\right)\right].$$

Then

$$\frac{\partial^2 q}{\partial n^2} = AC^*+A^*C+(BD^*+B^*D)\exp(-\sqrt{2}n)$$
$$+(BC^*+A^*D)\exp\left(-\frac{(1+\mathrm{i})}{\sqrt{2}}n\right)+(B^*C+AD^*)\exp\left(-\frac{(1-\mathrm{i})}{\sqrt{2}}n\right); \quad (3.9)$$

the term not involving n, AC^*+A^*C, can be discounted, because the sum of all such terms in (3.7) or (3.8) is zero. The solution of (3.9) that is bounded as $n\to\infty$ is then

$$q = E+\tfrac{1}{2}(BD^*+B^*D)\exp(-\sqrt{2}n)-\mathrm{i}(BC^*+A^*D)\exp\left(-\frac{(1+\mathrm{i})}{\sqrt{2}}n\right)$$
$$+\mathrm{i}(B^*C+AD^*)\exp\left(-\frac{(1-\mathrm{i})}{\sqrt{2}}n\right),$$

where E is a constant of integration which is not in general zero because it must be chosen so that $q = 0$ at $n = 0$. Hence, as $n\to\infty$,

$$q\to E = -\mathscr{R}(BD^*)-2\mathscr{I}(BC^*+A^*D). \quad (3.10)$$

The terms involving v_0 can be dealt with in a similar manner. If we write $u_{10}\to U(s)$, $w_{10}\to W(s)$ as $n\to\infty$, we can put all the results of the form (3.10) together to obtain

$$U(s) = \frac{1}{4}\left[\mathscr{R}\left\{3(u_{0w}^*-u_{0E}^*)\left[-\frac{\partial}{\partial s}(u_{0w}-u_{0E})+\frac{2}{3}w_{0E}\right]\right\}\right.$$
$$\left.+\mathscr{I}\left\{3(u_{0w}^*-u_{0E}^*)\left[\frac{\partial}{\partial s}(u_{0w}+u_{0E})+w_{0E}+\frac{2}{3}\kappa v_{0w}\right]\right\}\right], \quad (3.11)$$

$$W(s) = \frac{1}{4}\left[\mathscr{R}\left\{(u_{0w}^*-u_{0E}^*)\frac{\partial w_{0E}}{\partial s}+2w_{0E}\frac{\partial}{\partial s}(u_{0w}^*-u_{0E}^*)\right\}\right.$$
$$\left.+\mathscr{I}\left\{\left(\frac{\partial u_{0w}^*}{\partial s}+3\frac{\partial u_{0E}^*}{\partial s}\right)w_{0E}\right\}-3|w_{0E}|^2\right]. \quad (3.12)$$

These equations are in fact independent of the particular geometry of the problem. In our case w_{0E}, equation (3.3), is independent of s, so the first term on the right-hand side of (3.12) is zero.

4. The core steady-streaming problem

The non-zero mean velocities at the edge of the boundary layer, represented by $U(s)$ and $W(s)$, drive a steady-streaming flow in the core. The equations governing this flow are most conveniently expressed in Cartesian coordinates and are the same as (2.9)–(2.12) without the $\partial/\partial t$ terms. They can be made dimensionless by scaling lengths with a_0, velocities with the scale ϵU_0, derived from (2.15) and (3.4), p_0 with $\rho\epsilon^2 U_0^2$, and p_2 with $\rho\epsilon^2 U_0^2/a_0^2$. Thus (formally) ρ is set equal to 1 and ν is replaced by R_s^{-1} where R_s is the steady-streaming Reynolds number, given by

$$R_s = \frac{\epsilon U_0 a_0}{\nu} = \frac{U_0^2}{\Omega\nu} = \epsilon^2\alpha^2. \tag{4.1}$$

The boundary conditions are, as usual (Riley 1967), applied at the mean position of the wall, given by (2.1) with $a = a_0$, $b = b_0$ where a_0 and b_0 are constants. These conditions are

$$\left.\begin{aligned} u_x &= -U(s)\cos\psi(s), \\ u_y &= U(s)\sin\psi(s), \\ w_1 &= W(s), \end{aligned}\right\} \tag{4.2}$$

where ψ is given by (2.3) when θ is obtained from (2.4). The quantities $U(s)$ and $W(s)$ can be evaluated directly from (3.11) and (3.12) once the wall motion is completely specified; this is done for particular examples in the next section.

5. Specification of wall motion

The above is formulated so that any small-amplitude oscillation of the elliptical boundary can be incorporated. In order to obtain numerical results, however, it is necessary to consider particular wall motions. After having checked that we obtain Secomb's (1978) results when the cross-section is circular, we shall examine two special cases, as described in §1.

Case 1. Constant major axis

Here we set $a = a_0$ and let b vary, but we further insist that every element of the wall moves parallel to the minor axis so that θ = constant for each element (see (2.2)). In this case (2.6) and (3.2) give

$$u_{sE} = u_{sW} = \frac{b\dot{b}\sin\theta\cos\theta}{c},$$

while (2.5) and (3.3) give

$$u_{nW} = \frac{-\dot{b}a\sin^2\theta}{c},$$

$$w_{1E} = -\frac{\dot{b}}{b}.$$

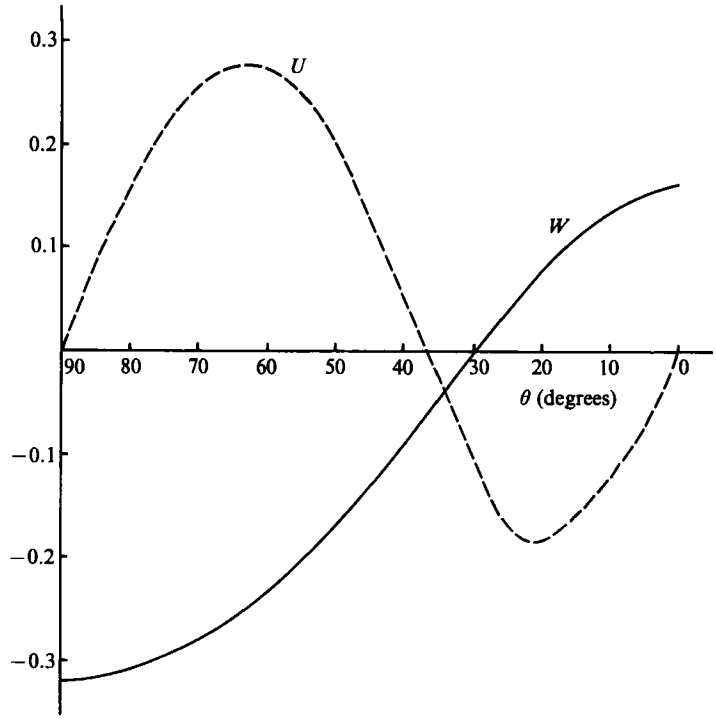

FIGURE 2. Graphs of the steady-streaming velocities at the edge of the Stokes layer, $U(s)$ (----) and $W(s)$ (——), against $\theta(s)$, calculated from (3.11) and (3.12) for the case of an inextensible boundary with $\bar{b}_0 = 0.8$.

If the oscillation is given in dimensional terms by

$$b = a_0\bar{b}_0(1+\epsilon e^{i\Omega t}), \quad \dot{b} = U_0\, i\bar{b}_0\, e^{i\Omega t},$$

then the transverse steady-streaming function $U(s)$ is identically zero, and the longitudinal function is constant:

$$W(s) = -\tfrac{3}{4}. \tag{5.1}$$

The secondary streaming problem is thus very similar to the two-dimensional case examined by Secomb (1978), for which $W = -\frac{3}{4}$ was also obtained. There is a difference, however, because in this case neither transverse component of velocity, u_x nor u_y, is zero, and w_1 depends on x as well as y (see §6).

Case 2. Inextensible wall

Here the value of s, (equation (2.4)), of any element of the wall remains constant at all times. Differentiating (2.4) then gives

$$\dot{\theta} = -\frac{1}{c(\theta)}\int_0^\theta \frac{a\dot{a}\sin^2\theta' + b\dot{b}\cos^2\theta'}{c(\theta')}\,d\theta', \tag{5.2}$$

where $c(\theta)$ is given by (2.7), so we see from (2.6) and (3.2) that u_{sW} and u_{sE} are no longer equal, with the result that $U(s)$ in (3.11) is not zero. We also note that a and b both vary with t, but not independently because the total perimeter of the tube remains constant. The ends of the major and minor axes are always at $\theta = 0$ and $\frac{1}{2}\pi$

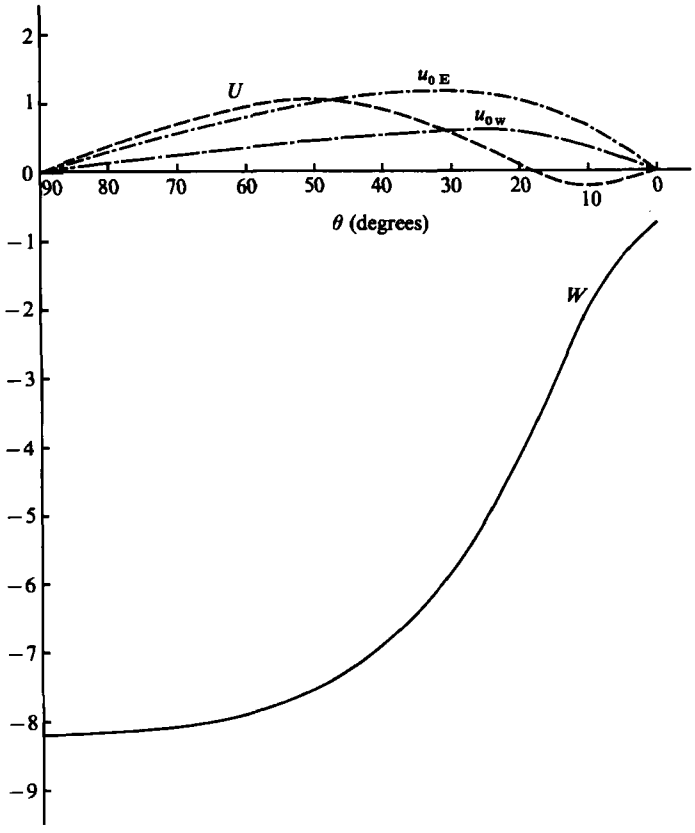

FIGURE 3. As figure 2, with $\bar{b}_0 = 0.4$, together with plots of $U_{0E}(s)$ and $U_{0W}(s)$ (dash-dot curves).

respectively, so $\dot{\theta}(0) = \dot{\theta}(\frac{1}{2}) = 0$; combined with the condition of inextensibility (5.2), applied at $\theta = \frac{1}{2}\pi$, this gives the following relation between $a(t)$ and $b(t)$:

$$\int_0^{\frac{1}{2}\pi} \frac{a\dot{a}\sin^2\theta + b\dot{b}\cos^2\theta}{c(\theta)}\,\mathrm{d}\theta = 0. \tag{5.3}$$

Thus, for a harmonic variation of a with time,

$$a = a_0(1 + \epsilon\, \mathrm{e}^{\mathrm{i}\Omega t}),$$

we obtain (dimensionally)

$$b = a_0\,\bar{b}_0(1 + \epsilon\mu\, \mathrm{e}^{\mathrm{i}\Omega t}),$$

where
$$\bar{b}_0^2\mu = -\int_0^{\frac{1}{2}\pi} \frac{\sin^2\theta'}{\bar{c}(\theta')}\,\mathrm{d}\theta' \Big/ \int_0^{\frac{1}{2}\pi} \frac{\cos^2\theta'}{\bar{c}(\theta')}\,\mathrm{d}\theta'. \tag{5.4}$$

and
$$\bar{c}(\theta) = (\sin^2\theta + \bar{b}_0^2\cos^2\theta)^{\frac{1}{2}}. \tag{5.5}$$

We see that $\dot{b}$ is negative when $\dot{a}$ is positive, so some elements of the wall move in while others move out.

The steady-streaming velocities $U(s)$ and $W(s)$ are now evaluated numerically from (3.11) and (3.12), using (2.4)–(2.7), (2.20), (3.2), (3.3) and (3.5). The results are plotted (against θ rather than s, for convenience) in figures 2, 3 and 4, for the values $\bar{b}_0 = 0.8$, 0.4 and 0.2 respectively; also plotted for comparison (on figure 3 only) are the

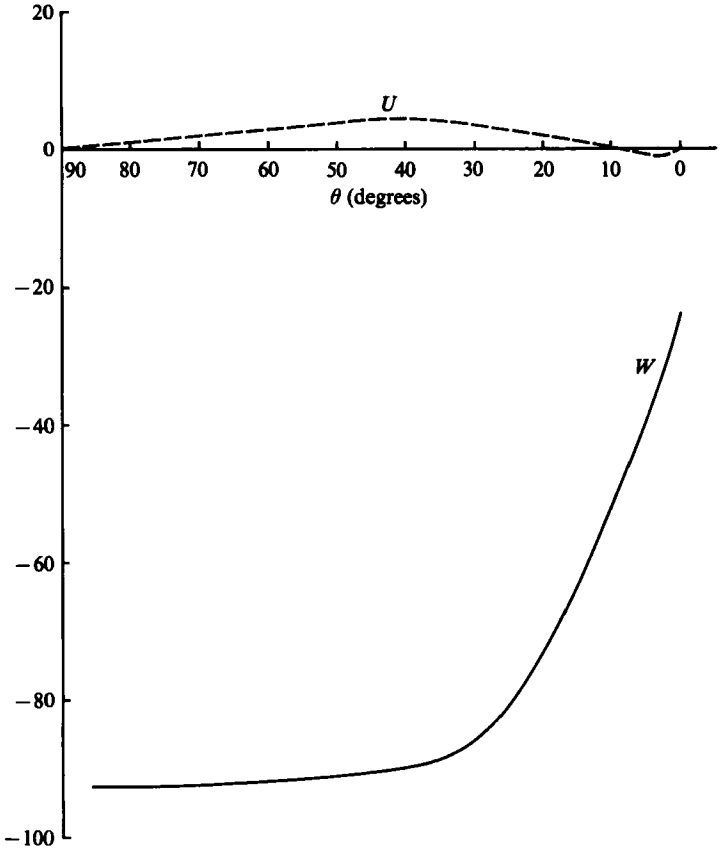

FIGURE 4. As figure 2, with $\bar{b}_0 = 0.2$.

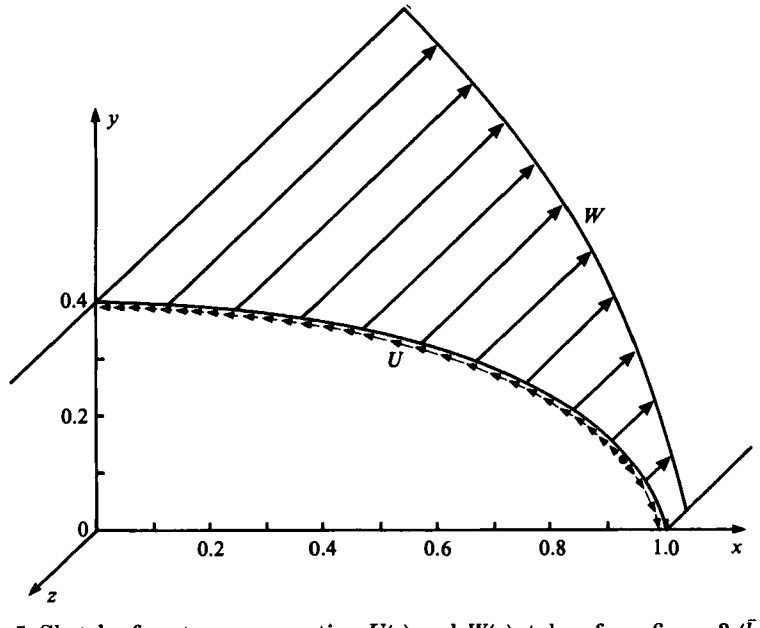

FIGURE 5. Sketch of vectors representing $U(s)$ and $W(s)$, taken from figure 3 ($\bar{b}_0 = 0.4$).

leading-order tangential velocity amplitudes, $u_{0\mathrm{w}}(s)$ and $u_{0\mathrm{E}}(s)$, both positive for all s (that is also true for the other values of $\bar{b}_0$). We can see that W is negative near the minor axis, which is consistent with the result from Case 1 because the flow is more two-dimensional there; this is particularly noticeable for the smallest value of $\bar{b}_0$ ($= 0.2$, figure 4) in which W remains almost constant for a considerable distance from the minor axis (until $\theta \approx \frac{1}{3}\pi$) before falling rapidly near the end of the major axis. As $\bar{b}_0$ increases W becomes less uniform near the minor axis and changes sign to become positive near the end of the major axis (small θ) when $\bar{b}_0$ exceeds a critical value somewhat in excess of 0.4 (see the end of §6 for further discussion). In all cases U is positive (towards the minor axis) near the minor axis and negative near the major axis. The distributions of W and U are sketched qualitatively in figure 5, for the case $\bar{b}_0 = 0.4$. We should note that the steady-streaming velocities are largest for the smallest value of $\bar{b}_0$, because the area change for a given major axis change is then greatest.

6. Steady streaming in the core: $R_\mathrm{s} \ll 1$

In the limit of small R_s (4.1) the steady-streaming motion in the core is a steady Stokes flow in which inertia is negligible. The governing equations, expressed in Cartesian coordinates and scaled as indicated in §4, therefore become

$$\nabla_1^2 w_1 = \bar{p}_2, \tag{6.1}$$

$$\nabla_1^2 u_x = \frac{\partial \bar{p}_0}{\partial x}, \quad \nabla_1^2 u_y = \frac{\partial \bar{p}_0}{\partial y}, \tag{6.2}$$

$$\frac{\partial u_x}{\partial x} + \frac{\partial u_y}{\partial y} + w_1 = 0, \tag{6.3}$$

where $(\bar{p}_0, \bar{p}_2)$ are equal to R_s multiplied by the mean values of p_0, p_2, and

$$\nabla_1^2 = \frac{\partial^2}{\partial x^2} + \frac{\partial^2}{\partial y^2}.$$

The boundary conditions (4.2) are applied on the undisturbed ellipse

$$x^2 + \frac{y^2}{\bar{b}_0^2} = 1. \tag{6.4}$$

The problem must be solved numerically in general.

In the present limit, the problem for w_1 can be separated from that for the secondary velocities u_x and u_y. For any given value of the constant $\bar{p}_2$, Poisson's equation (6.1) can be solved subject to $w_1 = W$ (known) on the ellipse. The actual value of $\bar{p}_2$ is determined from the condition that there must be no mean mass flow along the tube; i.e.

$$\left\langle \iint_A u_z \, \mathrm{d}x \, \mathrm{d}y \right\rangle = 0,$$

where the integral is taken over the time-dependent cross-section $A(t)$ and the angle brackets represent the time mean. Recalling that variables are expanded in the form (3.4) we can rewrite this as

$$\iint_{A_0} w_1 \, \mathrm{d}x \, \mathrm{d}y = -\left\langle \int w_{0\mathrm{E}}(s) \, \Delta n \, \mathrm{d}x \right\rangle, \tag{6.5}$$

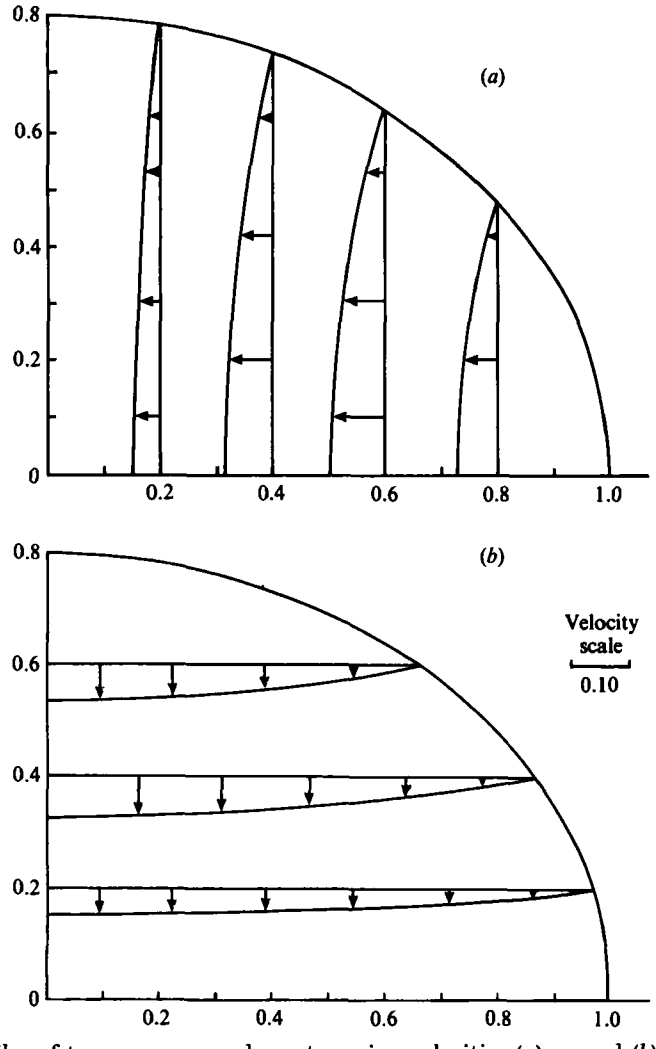

FIGURE 6. Profiles of transverse secondary streaming velocities (*a*) u_x and (*b*) u_y in the core, for the case of a constant major axis ($\bar{b}_0 = 0.8$).

where A_0 is the mean area of the ellipse, the integral on the right-hand side is taken round the perimeter and $\epsilon\Delta n$ is the (time-dependent) normal displacement of the element of boundary at s. In our case, however, w_{0E} is independent of s, from (3.3), and is proportional to $-\dot{A}$, so the right-hand side of (6.5) is proportional to $-\langle\dot{A}(A-A_0)\rangle$ which is zero; thus, eventually,

$$\iint_{A_0} w_1 \, dx \, dy = 0. \tag{6.6}$$

Numerically, the value of $\bar{p}_2$ and the solution for w_1 are obtained iteratively.

Knowing w_1, we can transform the problem for u_x and u_y into a conventional two-dimensional Stokes flow problem by writing

$$u_x = \frac{\partial \Psi}{\partial y} - \int_0^x w_1 \, dx, \quad u_y = -\frac{\partial \Psi}{\partial x}. \tag{6.7}$$

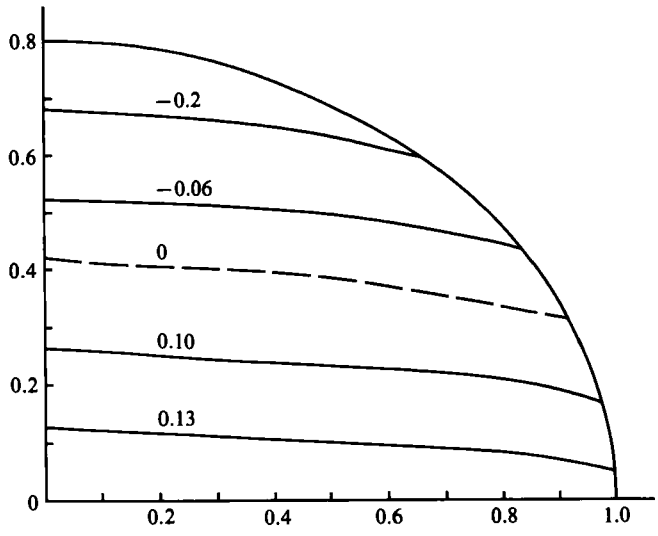

FIGURE 7. Contours of axial steady-streaming velocity w_1 in the core, for the case of an inextensible boundary with $\bar{b}_0 = 0.8$. The broken line is the null contour.

Equations (6.2) and (6.3) now reduce to the biharmonic equation

$$\nabla_1^4 \Psi = 0, \tag{6.8}$$

with boundary conditions (from (4.2))

$$\left.\begin{aligned} \frac{\partial \Psi}{\partial y} &= -U\cos\psi + \int_0^x w_1 \,\mathrm{d}x \equiv U_1(x,y), \\ \frac{\partial \Psi}{\partial x} &= -U\sin\psi \equiv V_1(x,y), \end{aligned}\right\} \tag{6.9}$$

applied on the ellipse (6.4). Note that (6.6) ensures no net flux across the boundary,

$$\oint (U_1 \,\mathrm{d}y - V_1 \,\mathrm{d}x) = 0,$$

a necessary condition on a two-dimensional incompressible flow. The numerical solution of (6.8) is achieved by splitting it into two (the 'stream function–vorticity' formulation):

$$\nabla^2 \Psi = \zeta, \quad \nabla^2 \zeta = 0,$$

and solving iteratively using a centred-difference scheme (Roache 1972). First, values of ζ on the boundary are guessed, then the problem for ζ is solved (using a Gauss–Seidel method) and next the problem for Ψ is solved, leading to a new estimate for ζ on the boundary. Iteration is continued until satisfactory convergence is achieved, defined by

$$\operatorname*{Max}_{i,j} |\, \Psi_{i,j}^m - \Psi_{i,j}^{m-1} \,| \leqslant \epsilon_0,$$

where the suffices refer to spatial position and m refers to iteration number; ϵ_0 was taken equal to 10^{-3}. Convergence was achieved after at most 160 iterations. The only

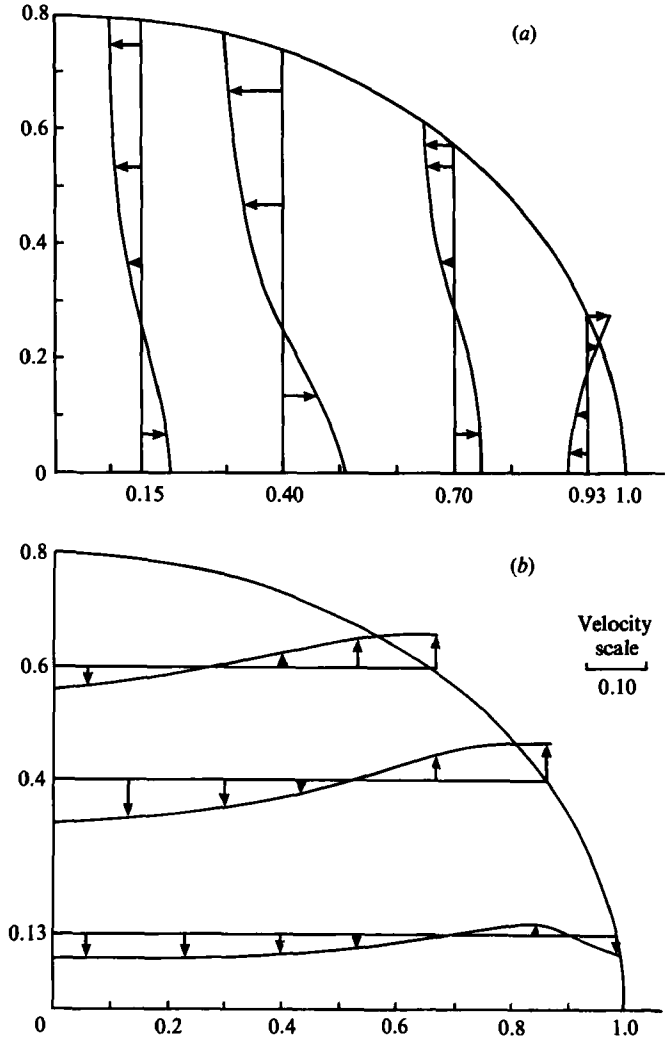

FIGURE 8. Profiles of transverse secondary streaming velocities (*a*) u_x and (*b*) u_y in the core, corresponding to the axial contours of figure 7 ($\bar{b}_0 = 0.8$).

difficult aspect of the computation was choosing a suitable interpolation scheme for evaluating ζ at the elliptical boundary. We have used the method adopted by Gupta & Manohar (1979). In this scheme, the values of ζ on the boundary are obtained from the values of Ψ inside the boundary, using a second-order interpolation formula.

In order to test our numerical program we first solved the problem of the axisymmetric tube for which the analytical solution was given by Secomb (1978). Here $U = 0$ and $W = -3$, the same everywhere on the circular boundary, and the solution is

$$w_1 = 3[1-2(x^2+y^2)], \quad \Psi = \tfrac{1}{2}xy(3-x^2-3y^2), \quad \bar{p}_2 = -24; \tag{6.10}$$

the transverse velocities are purely radial in this case. The computed values of w_1, u_x and u_y differed from those calculated from (6.10) by at most 1% when we took a grid size of $\Delta x = \Delta y = 0.1$.

An analytical solution to the problem is also available for the elliptical Case 1, of

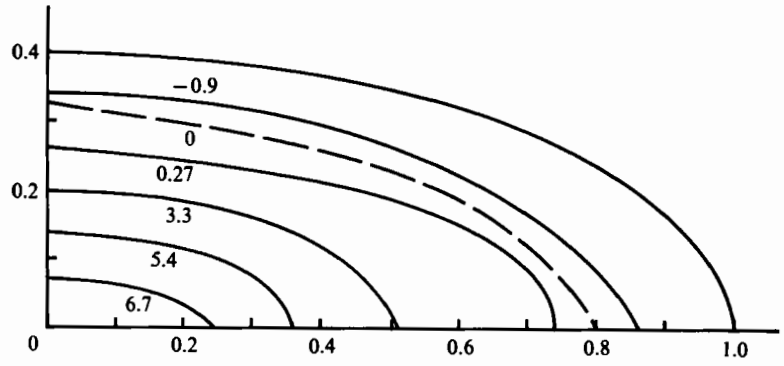

FIGURE 9. As figure 7, with $\bar{b}_0 = 0.4$.

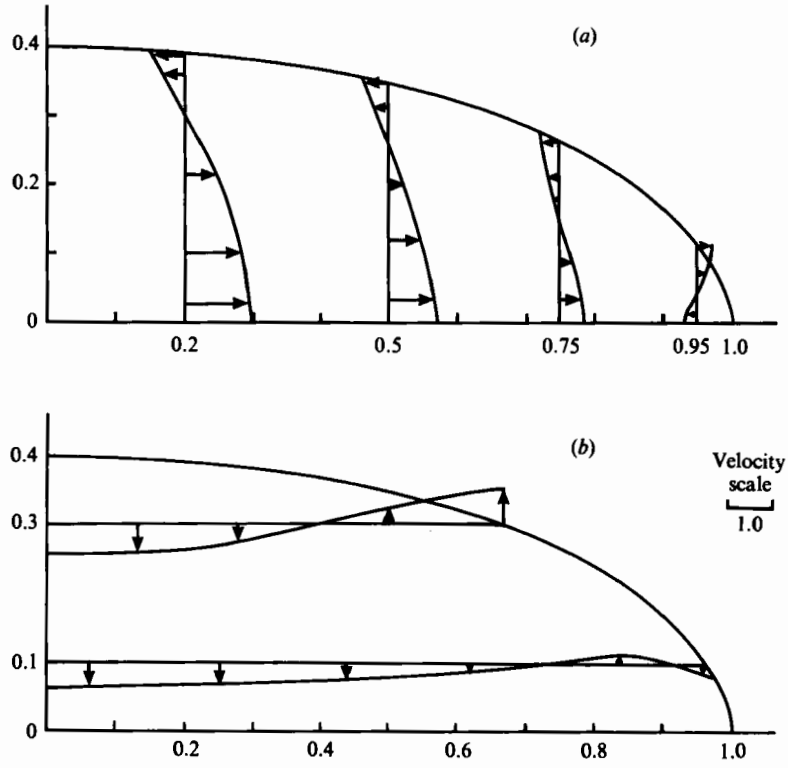

FIGURE 10. As figure 8, with $\bar{b}_0 = 0.4$.

constant major axis. Here again $U = 0$ and $W = \text{constant} = -\frac{3}{4}$, and in this case the solution is rather similar to (6.10):

$$w_1 = \frac{3}{4}\left[1-2\left(x^2+\frac{y^2}{\bar{b}_0^2}\right)\right], \quad \Psi = \tfrac{1}{8}xy\left(3-x^2-\frac{3y^2}{\bar{b}_0^2}\right), \quad \bar{p}_2 = -3\left(1+\frac{1}{\bar{b}_0^2}\right). \tag{6.11}$$

Once more, agreement between the computed and the analytical solutions was within 1 % for $\Delta x = 0.1$ and $\Delta y = 0.02$, even for values of $\bar{b}_0$ as low as 0.2. Profiles of the two transverse velocity components in this case are shown in figure 6; they are both directed towards the axes everywhere, as in the two-dimensional and axisymmetric

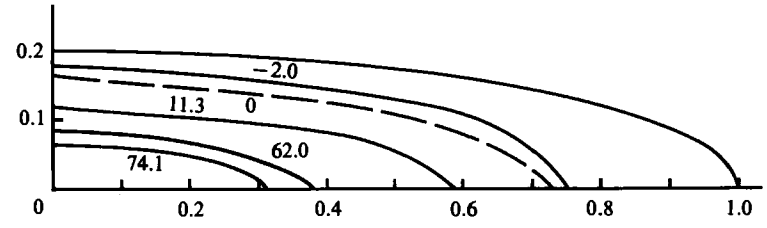

FIGURE 11. As figure 7, with $\bar{b}_0 = 0.2$.

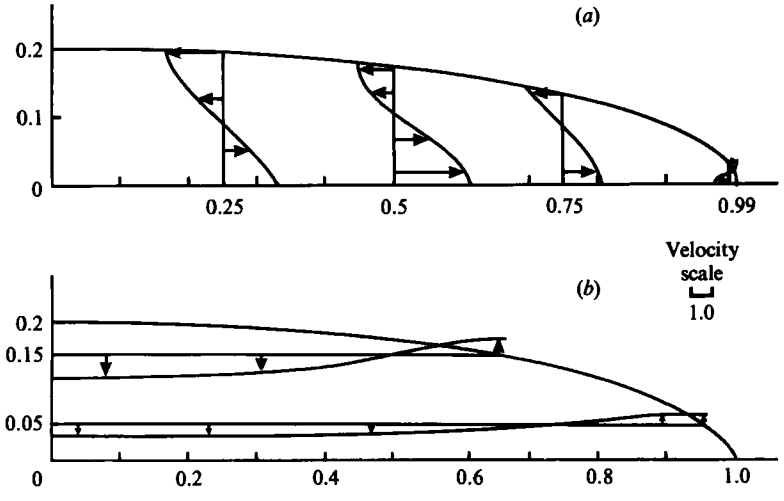

FIGURE 12. As figure 8, with $\bar{b}_0 = 0.2$.

cases. This is expected because the axial steady streaming, towards $z = 0$ near the wall, has to be turned away from $z = 0$ near the tube centreline.

No analytical solution is possible in Case 2 which, with an inextensible boundary, is the most realistic case examined. The numerical solution in this case is presented in figures 7–12 for three values of $\bar{b}_0$: 0.8, 0.4 and 0.2. Figures 7, 9 and 11 show contours of the axial steady-streaming velocity, w_1, while figures 8, 10 and 12 exhibit secondary velocity profiles. A number of features of these flow patterns deserve comment. For the least elliptical case ($\bar{b}_0 = 0.8$, figure 7) the axial velocity distribution in fact looks most two-dimensional, in that the contours of axial velocity are roughly parallel to the major axis and its profiles are fairly flat. As the tube's ellipticity becomes more pronounced, the contours of axial velocity tend to become more elliptical, and the region of negative axial velocity extends to the end of the major axis (figures 9 and 11; cf. figures 3 and 4). In each case the secondary flow in the first quadrant (figures 8, 10, 12) consists of one large counter-clockwise gyre with a small clockwise eddy near the end of the major axis, corresponding to the reversal of the driving velocity U near $\theta = 0$ (figures 2–4). These secondary flows are of course not divergence-free, because of their interaction with the axial motion.

7. Discussion

The solution of steady-streaming problems on general boundaries, with different tangential velocities at the wall and in the core flow outside the Stokes layer, is a cumbersome process. This was made very clear by Longuet-Higgins (1953) in a

general two-dimensional geometry. We have extended his formulation to the three-dimensional case of the present problem, which is not much more complicated because of the simple form of the z-dependence. The elliptical geometry combined with the three-dimensionality, however, makes the problem of computing the steady streaming in the core significantly more difficult than in the corresponding axisymmetric and two-dimensional geometries analysed by Secomb (1978). Except in the particularly simple Case 1, even the small-R_s solution must be solved numerically. In his examples, Secomb was able to solve both the small-R_s and the large-R_s problems analytically, and to show that the axial velocity profiles were qualitatively similar in each case.

There may be such similarity in our problem also, but we have not as yet solved the large-R_s problem even in the simple Case 1. We formulate it on the assumption that, as in Secomb's problems, mean vorticity is distributed throughout the core and is not confined to thin boundary layers. We thus seek an inviscid, rotational flow, and the governing equations (from §4) can be reduced to

$$(\boldsymbol{u}\cdot\boldsymbol{\nabla})\,w_1 = -w_1^2 - p_2, \tag{7.1}$$

$$(\boldsymbol{u}\cdot\boldsymbol{\nabla})\,\zeta = +w_1\,\zeta, \tag{7.2}$$

$$\boldsymbol{\nabla}\cdot\boldsymbol{u} = -w_1, \tag{7.3}$$

$$\zeta = \frac{\partial u_y}{\partial x} - \frac{\partial u_x}{\partial y}, \tag{7.4}$$

where $\boldsymbol{u} = (u_x, u_y)$ is the two-dimensional velocity field in the transverse plane, p_2 is a constant and $\boldsymbol{\nabla}$ is the two-dimensional gradient operator. Both $\boldsymbol{u}$ and w_1 are functions only of (x, y). The boundary conditions are still given by (4.2), applied on the ellipse (6.4), and we note that they imply the condition

$$\boldsymbol{u}\cdot\boldsymbol{n} = 0 \tag{7.5}$$

on the boundary. The constraint (6.6) on w_1 is also still true.

The only conclusion that we can draw from this problem is an expression for the mean pressure term p_2: integrate (7.1) across the tube cross-section A_0, using (7.3) and (7.5), to obtain

$$p_2 = -\frac{2}{A_0}\int\int w_1^2 \,\mathrm{d}x\,\mathrm{d}y. \tag{7.6}$$

Thus p_2 is negative, and the mean pressure in the core ($\propto z^2 p_2$) is highest near $z = 0$, whatever the distribution of U and W at the wall. This is consistent with the small-R_s solutions given by (6.10) and (6.11), and can be explained as follows. The steady-streaming velocity at the wall is directed on average towards $z = 0$, so the pressure must be highest there in order for its gradient to drive a compensating flow away from $z = 0$. This pressure gradient has to overcome viscous forces in the small-R_s case, and inertial forces (inward-moving fluid particles are decelerated and re-accelerated outwards) in the large-R_s case.

This conclusion suggests that oscillations in an elastic tube would generate a (mean) bulge in the vicinity of $z = 0$, whatever the value of R_s, and this would tend to counter the Bernoulli effect which is usually associated with collapse. However, once a bulge or localized collapse has occurred, the present theory will become invalid and non-parallel tube effects such as flow separation will have to be considered. Thus two problems are immediately suggested for future research. One is the numerical solution

of the core steady-streaming problem, formulated in §4, for finite R_s. The other is the generalization of the present work to include non-parallel and elastic walls. These are both challenging problems which are currently under investigation.

We are grateful to the UK Overseas Development Administration for their support of the collaborative research project on Physiological Fluid Dynamics, between IIT-Delhi, Cambridge University and Imperial College, London, under the terms of which Dr Padmanabhan spent a year in Cambridge from March 1984.

REFERENCES

CANCELLI, C. & PEDLEY, T. J. 1985 A separated-flow model for collapsible-tube oscillations. *J. Fluid Mech.* **157**, 375–404.

CONRAD, W. A. 1969 Pressure–flow relationships in collapsible tubes. *IEEE Trans. Bio-med. Engng. BME*-16, 284–295.

GUPTA, M. M. & MANOHAR, R. P. 1979 Boundary approximations and accuracy in viscous flow computations. *J. Comp. Phys.* **31**, 265–288.

LONGUET-HIGGINS, M. S. 1953 Mass transport in water waves. *Phil. Trans. R. Soc. Lond.* A **245**, 535–581.

LYNE, W. H. 1971 Unsteady viscous flow in a curved pipe. *J. Fluid Mech.* **45**, 13–31.

MORENO, A. H., KATZ, A. I., GOLD, L. D. & REDDY, R. V. 1970 Mechanics of distension of dog veins and other very thin-walled tubular structures. *Circ. Res.* **27**, 1069–1080.

PEDLEY, T. J. 1980 *The Fluid Mechanics of Large Blood Vessels.* Cambridge University Press.

RAYLEIGH, LORD 1883 On the circulation of air observed in Kundt's tubes, and on some allied acoustical problems. *Phil. Trans. R. Soc. Lond.* **175**, 1–21.

RILEY, N. 1967 Oscillatory viscous flows. Review and extension. *J. Inst. Maths Applics* **3**, 419–434.

ROACHE, P. J. 1972 *Computational Fluid Dynamics.* Albuquerque, Hermosa.

SECOMB, T. W. 1978 Flow in a channel with pulsating walls. *J. Fluid Mech.* **88**, 273–288.